

Preparation, Spectroscopy, and Photochemistry of Monometallic and Bimetallic Ruthenium(II) Ammine Complexes of 2,2'-Bipyrimidine

RONALD R. RUMINSKI and JOHN D. PETERSEN*

Received March 9, 1982

The monometallic and bimetallic complexes of ruthenium(II) amines bound to 2,2'-bipyrimidine, $(\text{NH}_3)_4\text{Ru}(\text{bpym})^{2+}$ and $((\text{NH}_3)_4\text{Ru})_2(\text{bpym})^{4+}$, have been prepared and characterized. Electronic spectroscopy of the monometallic complex shows an intense metal-to-ligand charge-transfer (MLCT) band in the visible region centered at 402 nm while the bimetallic complex has intense absorption bands (MLCT in nature) at 424 and 697 nm. Cyclic voltammetry of the monometallic complex in aqueous solution shows a reversible one-electron oxidation with $E^\circ = +0.756$ V vs. NHE. The bimetallic complex shows a reversible one-electron oxidation with $E^\circ = +0.830$ V. A second one-electron oxidation of the bimetallic complex is quasireversible ($E^\circ \approx +1.02$ V) and results in the breakdown of the fully oxidized species to $(\text{NH}_3)_4\text{Ru}(\text{bpym})^{3+}$ and $(\text{NH}_3)_4\text{Ru}(\text{H}_2\text{O})_2^{3+}$. Photolysis of the bimetallic complex at 436 or 691 nm leads to only slight degradation of the complex with an upper limit $\Phi < 5 \times 10^{-4}$ mol/einstein.

Introduction

Previous studies in our laboratories, as well as others, have shown that Ru(II) amines and cyanoferrate(II) complexes containing unsaturated nitrogen donor ligands have photo-substitution quantum yields that can vary by 3 orders of magnitude at these highly absorbing centers by tuning the relative energies of the metal-to-ligand charge-transfer (MLCT) and the ligand field (LF) excited states.¹⁻⁴ The emphasis of our recent work in this area has been to synthesize a photon-absorbing (antenna) fragment $(\text{NH}_3)_4\text{RuL}^{2+}$ and couple this to a second (reactive) metal center with the requirements that (1) $(\text{NH}_3)_4\text{RuL}^{2+}$ be inert to photosubstitution reactions and (2) L also function as a highly communicative bridge to a second metal center. 2,2'-Bipyrimidine was selected as an appropriate chelate (L) because as a bridging ligand it is bidentate with respect to both the Ru antenna and reactive metal fragment and therefore is less susceptible to either thermal or photochemical bridge rupture. Additionally, the 2,2'-bipyrimidine ring systems can be expected to possess a large amount of delocalized π bonding, similar to the 2,2'-bipyridine, 1,10-phenanthroline, or pyrazine unsaturated ring systems. Some evidence for more efficient bidentate communication between Ru(II) metal centers has been shown by the previously reported $((\text{bpy})_2\text{Ru})_2\text{L}^{4+}$ (L = 2,2'-bipyrimidine, 4,4'-dimethyl-2,2'-bipyrimidine; bpy = 2,2'-bipyridine) complexes.^{6,7}

We report here the synthesis, electronic absorption spectra, cyclic voltammetry, and photochemistry of $((\text{NH}_3)_4\text{Ru})_n(\text{bpym})^m$ (where bpym = 2,2'-bipyrimidine, $n = 1, 2$, and $m = 2, 4$) complexes.

Experimental Section

Materials. Analytical reagent grade compounds were used for all preparations described in this work. Water used as the solvent for synthesis, photolysis, and electrochemistry was redistilled from alkaline permanganate in an all-glass apparatus. Elemental analysis were performed by Atlantic Microlab, Atlanta, GA.

Synthesis. The synthesis of $[(\text{NH}_3)_4\text{Ru}(\text{bpym})](\text{ClO}_4)_2$ required several intermediate preparations. The $[\text{Ru}(\text{NH}_3)_5\text{Cl}]\text{Cl}_2$ intermediate was prepared by following previous literature reports.⁸ One gram

of $[\text{Ru}(\text{NH}_3)_5\text{Cl}]\text{Cl}_2$ was converted to the air-stable $[\text{Ru}(\text{NH}_3)_5\text{H}_2\text{O}](\text{TFMS})_3$ (HTFMS = trifluoromethanesulfonic acid) complex according to previous reports.^{9,10} The pale white solid $[\text{Ru}(\text{NH}_3)_5\text{H}_2\text{O}](\text{TFMS})_3$ had an electronic absorption spectrum that was in good agreement with the previously reported spectrum.^{11,12}

Tetraammine(2,2'-bipyrimidine)ruthenium(II) perchlorate was prepared by a modification in the preparation of tetraammine(2,2'-bipyridine)ruthenium(II) perchlorate.¹³ A 0.1-g sample of $[\text{Ru}(\text{NH}_3)_5\text{H}_2\text{O}](\text{TFMS})_3$ was dissolved in 25 mL of 100% ethanol and a 10-fold molar excess of 2,2'-bipyrimidine (Alfa Chemicals) and deaerated for 15 min with argon. Zn(Hg) amalgam was then added and the solution stirred for 1.5 h under argon. Addition of ether precipitated the crude red product. Following collection by filtration, the precipitate was redissolved in a minimum volume of water, washed with chloroform to remove excess bipyrimidine, and reprecipitated by addition of saturated aqueous NaClO_4 . The dark red complex was washed with 100% ethanol and then with ether and dried under vacuum; yield 51 mg (64%). Anal. Calcd for $\text{C}_8\text{H}_{18}\text{N}_8\text{Cl}_2\text{O}_8\text{Ru}$: C, 18.25; H, 3.42; N, 21.29. Found: C, 18.09; H, 3.49; N, 21.13.

The bis(tetraammineruthenium(II)) 2,2'-bipyrimidine perchlorate bimetallic complex was prepared in a manner similar to that for the monometallic complex, except that a 2-fold molar excess of $[\text{Ru}(\text{NH}_3)_5\text{H}_2\text{O}](\text{TFMS})_3$ to 2,2'-bipyrimidine was used. After final washing and drying of the green product with ethanol and ether, a sample was dissolved in H_2O and eluted down a Sephadex (C-25) column (which had previously separated a mixture of monometallic and bimetallic complexes) to confirm that negligible monometallic complex was formed; yield 37 mg (54%). Anal. Calcd for $\text{C}_8\text{H}_{30}\text{N}_{12}\text{Cl}_4\text{O}_{16}\text{Ru}_2$: C, 10.74; H, 3.36; N, 18.79. Found: C, 11.10; H, 3.39; N, 17.95.

Instrumentation. All electronic spectra were recorded on a Bausch & Lomb Spectronic 2000 dual-beam spectrophotometer using matched quartz cells.

Cyclic voltammograms were obtained with a Bioanalytical Systems instrument (Model CV 1B-120). The platinum-disk working electrode (1.5 mm diameter) was polished with 1- μm alumina powder prior to each series of scans. A silver chloride coated silver wire in 0.10 M KCl served as a reference electrode (nominally +0.288 V vs. NHE) and was separated from the working solution by an agar bridge filled with KCl. A short piece of 14-gauge platinum wire was used as an auxiliary electrode. The cell was constructed from a 60° glass funnel sealed at the stem. This arrangement permitted recording of voltammograms with as little as 1 mL of solution. All scans were recorded in deoxygenated 0.10 M KCl solution with N_2 blowing over the top during the scan. Scan rates ranging from 50 to 150 mV/s were used. The potentials reported for the redox couples are estimates obtained by averaging the anodic and cathodic peak potentials and referenced to NHE. They are not corrected for junction potential.

- (1) Malouf, G.; Ford, P. C. *J. Am. Chem. Soc.* **1977**, *99*, 7213.
- (2) Malouf, G.; Ford, P. C. *J. Am. Chem. Soc.* **1974**, *96*, 601.
- (3) Figard, J. E.; Petersen, J. D. *Inorg. Chem.* **1978**, *17*, 1059.
- (4) Gelroth, J. A.; Figard, J. E.; Petersen, J. D. *J. Am. Chem. Soc.* **1979**, *101*, 3649.
- (5) Zwickel, A. M.; Creutz, C. *Inorg. Chem.* **1971**, *10*, 2395.
- (6) Dose, E. V.; Wilson, L. J. *Inorg. Chem.* **1978**, *17*, 2660.
- (7) Hunziker, M.; Ludi, A. *J. Am. Chem. Soc.* **1977**, *99*, 7370.
- (8) Allen, A. D.; Bottomly, F.; Harris, R. O.; Reinsalu, V. P.; Senoff, C. V. *J. Am. Chem. Soc.* **1967**, *89*, 5595.

- (9) Stanbury, D. M.; Haas, O.; Taube, H. *Inorg. Chem.* **1980**, *19*, 518.
- (10) Diamond, S. E.; Taube, H. *J. Am. Chem. Soc.* **1975**, *97*, 5921.
- (11) Broomhead, J. A.; Basolo, F.; Pearson, R. G. *Inorg. Chem.* **1964**, *3*, 826.
- (12) Taube, H.; Endicott, J. F. *J. Am. Chem. Soc.* **1962**, *84*, 4984.
- (13) Brown, G. M.; Sutin, N. *J. Am. Chem. Soc.* **1979**, *101*, 883.

Table I. Absorption Spectra Maxima and Extinction Coefficients for Some Ru(II) Complexes

complex	λ_{\max} , nm	$10^4 \epsilon_{\max}$, $M^{-1} \text{ cm}^{-1}$	ref
$(\text{NH}_3)_4\text{Ru}(\text{bpym})^{2+}$	402	0.84	<i>a</i>
	567	0.20	
$((\text{NH}_3)_4\text{Ru})_2(\text{bpym})^{4+}$	424	1.8	<i>a</i>
	697	0.40	
$(\text{NH}_3)_4\text{Ru}(\text{bpy})^{2+}$	366	0.55	13
	522	0.33	
$(\text{NH}_3)_4\text{Ru}(\text{phen})^{2+}$	265	3.5	13
	471	0.27	
$(\text{bpy})_2\text{Ru}(\text{bpym})^{2+}$	398 ^b	...	
	415	1.13	6, 7
	475 ^b	...	
$((\text{bpy})_2\text{Ru})_2(\text{bpym})^{4+}$	408	3.1	6, 7
	560 ^b	...	
	606	0.76	
$(\text{bpy})_3\text{Ru}^{2+}$	423 ^b	...	17
	452	1.4	
$(\text{bpym})_3\text{Ru}^{2+}$	331	1.48	7
	412	0.76	
	452	0.74	

^a This work. ^b Shoulder.

Photolysis Procedures. Irradiation of samples was accomplished with a continuous-beam photolysis apparatus consisting of an Oriol universal arc source lamp with a 200-W high-pressure Hg lamp, 1 in. diameter Oriol mercury-line interference filters (436, 691 nm), and ESCO A-1 4 in. focal length fused quartz collimating lens and a hollow brass thermostated cell compartment (controlled by a Forma Temp Jr. constant-temperature circulating bath) all mounted on an Ealing 22-6894 optical bench. Usable intensities of this apparatus as measured by ferrioxalate and/or Reinecke actinometry at 436 and 691 nm were 5.8×10^{17} and 4.8×10^{16} quanta/min, respectively.^{14,15}

The solutions used for the photolysis studies were generated and transferred to absorption cells under argon gas with use of a previously described apparatus and technique.¹⁶ Samples were irradiated for time periods ranging from 2 to 6 h. Spectroscopic changes in the sample were determined at 1-h intervals throughout the photolysis at the wavelength of irradiation and the wavelength of the MLCT band of the starting complex for use in calculating the quantum yield. All spectroscopic measurements were corrected for thermal reactions by the use of a dark sample.

The quantum yield was calculated according to the formula

$$\Phi_t = [((\Delta A)V)/(I(\Delta\epsilon))]/(I_0 t F)$$

where ΔA is the change in absorbance at the monitoring wavelength from time 0 to time t (t in min), $\Delta\epsilon$ is the extinction coefficient difference of the starting complex and the final product ($M^{-1} \text{ cm}^{-1}$), V is the volume of the photolysis cell (L), l is the path length of the photolysis cell (cm), I_0 is the incident light intensity (einsteins/min), t is the irradiation time (min), and F is the average fraction of light absorbed at the irradiation wavelength over the time period t .

The Φ_t value for each time period of the photolysis reaction was plotted vs. percent reaction and the initial quantum yield obtained by extrapolation to 0% reaction.

Results and Discussion

The band maxima and extinction coefficients in the electronic spectrum for $(\text{NH}_3)_4\text{Ru}(\text{bpym})^{2+}$, $((\text{NH}_3)_4\text{Ru})_2(\text{bpym})^{4+}$, and similar Ru(II) complexes are summarized in Table I. The absorption spectrum of $(\text{NH}_3)_4\text{Ru}(\text{bpym})^{2+}$ is dominated by an intense band at 402 nm ($\epsilon = 8.4 \times 10^3 M^{-1} \text{ cm}^{-1}$) with a distinct longer wavelength shoulder at 567 nm ($\epsilon = 2.0 \times 10^3 M^{-1} \text{ cm}^{-1}$). On the basis of intensity, and by analogy to previously reported Ru(II) ammine complexes, the origin of these bands is also probably MLCT in charac-

Table II. Absorption Maxima for Some Monometallic and Bimetallic Ru(II) Complexes^a

monometallic complex	λ_{\max} , nm	bimetallic complex	λ_{\max} , nm	ref
$(\text{NH}_3)_5\text{Ru}(\text{pyz})^{2+}$	472	$((\text{NH}_3)_5\text{Ru})_2(\text{pyz})^{4+}$	547	19
$(\text{bpy})_2\text{ClRu}(\text{pyz})^+$	478	$((\text{bpy})_2\text{ClRu})_2(\text{pyz})^{2+}$	513	25, 19
$(\text{NH}_3)_3\text{Ru}(\text{bpym})^{2+}$	424	$((\text{NH}_3)_3\text{Ru})_2(\text{bpym})^{4+}$	442	18

^a pyz = pyrazine, bpym = 4,4'-bipyridylamine.

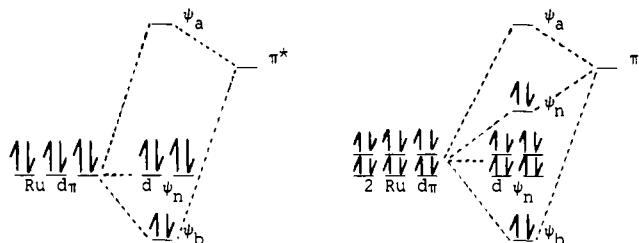


Figure 1. Molecular orbital diagram for monometallic and bimetallic Ru(II) complexes.

ter.^{5-7,18-22} The λ_{\max} and ϵ values are similar, although red shifted, to the value for the monometallic $(\text{NH}_3)_4\text{Ru}(\text{bpy})^{2+}$ complex.

The lower energy of the $(\text{NH}_3)_4\text{Ru}(\text{bpym})^{2+}$ vs. the $(\text{NH}_3)_4\text{Ru}(\text{bpy})^{2+}$ complex suggests that the $\pi^* \leftarrow d\pi$ transition for bpym is lower than for bpy. Qualitatively, this fits into the previously established pattern of lowering the $\pi^* \leftarrow d\pi$ transition energy as electron-withdrawing groups are substituted in and on the nitrogen aromatic rings.^{5,23} Furthermore, these results are not surprising since molecular orbital calculations indicate the bpym π^* LUMO lies lower in energy than the corresponding bpy LUMO. Thus, the net result of the lower energy bpym LUMO is to decrease the energy of the $\pi^* \leftarrow d\pi$ transition, as observed.

The visible absorption spectrum of $((\text{NH}_3)_4\text{Ru})_2(\text{bpym})^{4+}$ exhibits two bands. The higher energy band occurs at 424 nm ($\epsilon = 1.8 \times 10^4 M^{-1} \text{ cm}^{-1}$), with a lower energy band at 697 nm ($\epsilon = 4.0 \times 10^3 M^{-1} \text{ cm}^{-1}$). Owing to the similarity of peak position and intensity of the bimetallic complex to those of the corresponding monometallic complex, the more intense bimetallic band is also probably MLCT in character. The lower energy absorption at 697 nm is similar in position and intensity to the low-energy absorption of the previously reported $((\text{bpy})_2\text{Ru})_2(\text{bpym})^{4+}$ bimetallic complex.^{6,7}

In both $((\text{NH}_3)_4\text{Ru})_2(\text{bpym})^{4+}$ complexes, the absorption maxima are at lower energy in comparison to those of the $((\text{bpy})_2\text{Ru})_2(\text{bpym})^{4+}$ analogues. This result can be explained by the fact that the bpy π^* LUMO participates in Ru(II)-bpy back-bonding. The stabilization of the Ru(II) $d\pi$ orbitals by the bpy thus increases the MLCT energy as compared with the non- π -back-bonding ammine ligands. The fact that the bimetallic absorption maxima for $((\text{NH}_3)_4\text{Ru})_2(\text{bpym})^{4+}$ are at lower energy than the $(\text{NH}_3)_4\text{Ru}(\text{bpym})^{2+}$ monometallic absorption maxima agrees with the pattern for other monometallic and bimetallic com-

- (14) Wegner, E. E.; Adamson, A. W. *J. Am. Chem. Soc.* **1966**, *88*, 394.
 (15) Hatchard, C. G.; Parker, C. A. *Proc. R. Soc. London, Ser. A* **1956**, *235*, 518.
 (16) Ford, P. C.; Kuempel, J. R.; Taube, H. *Inorg. Chem.* **1968**, *7*, 1976.
 (17) Lin, C. T.; Böttcher, W.; Chou, M.; Creutz, C.; Sutin, N. *J. Am. Chem. Soc.* **1976**, *98*, 6536.

- (18) Sutton, J. E.; Taube, H. *Inorg. Chem.* **1981**, *20*, 3125.
 (19) Creutz, C.; Taube, H. *J. Am. Chem. Soc.* **1973**, *95*, 1086.
 (20) Alvarez, V. E.; Allen, R. J.; Matsubara, T.; Ford, P. C. *J. Am. Chem. Soc.* **1974**, *96*, 7686.
 (21) Powers, M. J.; Meyer, T. J. *J. Am. Chem. Soc.* **1980**, *102*, 1289.
 (22) Sutton, J. E.; Sutton, P. M.; Taube, H. *Inorg. Chem.* **1979**, *18*, 1010.
 (23) Ford, P. C.; Rudd, D. F.; Gaunders, R.; Taube, H. *J. Am. Chem. Soc.* **1968**, *90*, 1187.
 (24) Our CNDO calculations show the bpym LUMO at 0.0949 hartree vs. the bpy LUMO at 0.1086 hartree.
 (25) Callahan, R. W.; Keene, F. R.; Meyer, T. J.; Salmon, D. J. *J. Am. Chem. Soc.* **1977**, *99*, 1064.
 (26) Meyer, T. J. *Acc. Chem. Res.* **1978**, *11*, 94.
 (27) Brown, David, Ed. *NATO Adv. Study Inst. Ser., Ser. C* **1980**, *58*.

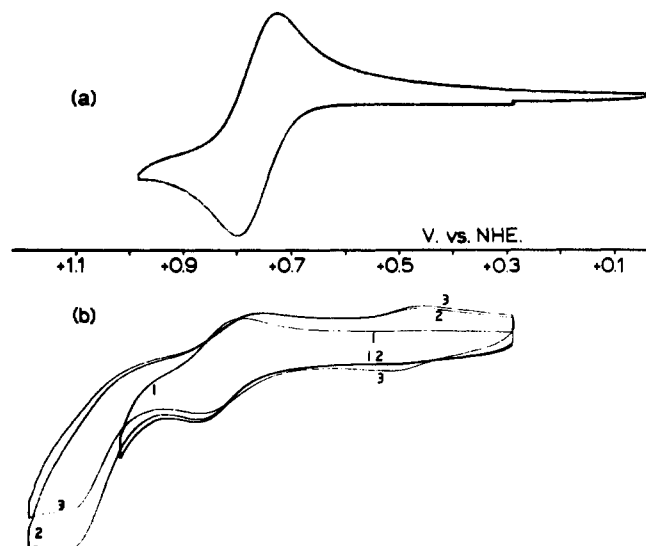


Figure 2. (a) Cyclic voltammogram of $(\text{NH}_3)_4\text{Ru}(\text{bpym})^{2+}$ in 0.10 M KCl vs. NHE. (b) Cyclic voltammogram of $((\text{NH}_3)_4\text{Ru})_2(\text{bpym})^{4+}$ in 0.10 M KCl vs. NHE: scan 1, reversible one-electron oxidation of the complex $[2,2] \rightleftharpoons [2,3]$; scan 2, two one-electron oxidation waves followed by quasi-reversible reduction (note the reduction competitive with bond cleavage as shown by migration of the $[2,3] \rightleftharpoons [2,2]$ reduction toward monometallic complex $2+/3+$ reduction and growth of the reduction due to $(\text{NH}_3)_4\text{Ru}(\text{H}_2\text{O})_2^{3+/2+}$); scan 3, repeat of scan 2 with smaller peaks in oxidation indicating the decomposition reaction is bridge cleavage and not NH_3 substitution (see text).

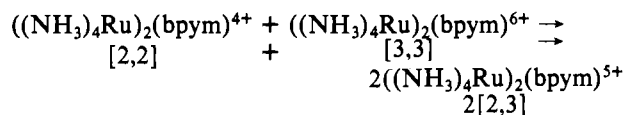
plexes (Table II). Reasons for this shift have been previously explained by consideration of the Ru(II) $d\pi$ and aromatic π^* LUMO interaction (Figure 1).^{5,19} Coupling of the Ru(II) orbitals with the ligand π LUMO creates a set of bonding (ψ_b), nonbonding (ψ_n), and antibonding (ψ_a) orbitals. The presence of the nonbonding (ψ_n) HOMO in the bimetallic complex gives rise to a lower energy transition than in the corresponding monometallic complex.

The cyclic voltammetry of the $(\text{NH}_3)_4\text{Ru}(\text{bpym})^{2+}$ complex shows a single reversible wave when scanned from 0.0 to +0.99 V (vs. NHE) (Figure 2a). The $E_{1/2}$ value is +0.756 V and is indicative of the one-electron $2+/3+$ oxidation-reduction couple. Electrochemistry of $((\text{NH}_3)_4\text{Ru})_2(\text{bpym})^{4+}$ was completed in two steps. When the complex was scanned from 0.0 to +0.99 V, the reversible one-electron $4+/5+$ oxidation-reduction couple occurred at $E_{1/2} = +0.830$ V. This trace was reproducible through several scans with no apparent sample decomposition. When the oxidation potential was extended to +1.19 V, a second quasi-reversible oxidation peak occurred at $E_{1/2} = +1.02$ V due to the $5+/6+$ oxidation and reduction (Figure 2b). The $E_{1/2}$ value of +1.02 V was estimated from the first scan and assumes only small amounts of reactant decomposition at the platinum electrode surface. Due to a steep decrease of the base line at +0.90 V, and the quasi-reversibility, the anodic and cathodic waves were usually separated by more than 60 mV. After the scan through the more positive potential, the reduction peak for the $5+/4+$ reduction was shifted to less positive potential, indicating some reaction of the fully oxidized $6+$ species had occurred, although the shift does not correspond to complete monometallic complex formation. Subsequent scans through the $4+/5+/6+$ oxidation produced further current loss due to product decomposition, although no further changes in $E_{1/2}$ potentials. Since

the $5+/6+$ oxidation peak does not change potential, the products probably do not include any substituted bimetallic complexes such as $(\text{NH}_3)_3(\text{H}_2\text{O})\text{Ru}(\text{bpym})\text{Ru}(\text{NH}_3)_4^{6+}$, which would have a different oxidation potential. It is more likely the products are a mixture of the $(\text{NH}_3)_4\text{Ru}(\text{bpym})^{3+}$ and $(\text{NH}_3)_4\text{Ru}(\text{H}_2\text{O})_2^{3+}$ complexes, which arise from bridge rupture of the fully oxidized bimetallic complex.

The separation between $E_{1/2}(4+/5+)$ and $E_{1/2}(5+/6+)$ of 190 mV is comparable with the 170- and 180-mV differences observed for the similar bidentate $((\text{bpy})_2\text{Ru})_2(\text{L})^{4+}$ (where $\text{L} = 4\text{-}4'\text{-Me}_2\text{bpy}$ or bpy) complexes.^{6,7} The slight increase in $\Delta E_{1/2}$ may reflect a greater amount of electron delocalization between the two Ru(II) centers by replacing the bpy ligands with NH_3 . This substitution eliminates the electron back-donation from the Ru(II) to the nonbridging ligand and thus increases electron delocalization to the bridging chelate ring systems. The $\Delta E_{1/2}$ difference of 190 mV for the bpym bridged complexes represents a considerable increase of Ru(II)-Ru(III) communication over that of most monodentate-ring-bridged complexes ($\Delta E_{1/2} = 50\text{-}80$ mV) with the exception of the Creutz-Taube pyrazine-bridged bimetallic complex ($\Delta E_{1/2} = 390$ mV).^{18,19}

With distinctly separable $E_{1/2}$ values, the comproportionation constant K_{com} can be calculated from electrochemical data. With use of the $E_{1/2}$ values obtained, K_{com} for the comproportionation equilibrium



is calculated to be 1.50×10^3 . The value is much larger than the statistical value of 4 and represents a high degree of stability of the mixed-valence species as compared with other Ru amine systems.

Irradiation of the bimetallic complex was performed at 436 and 691 nm, which lie close to absorption maxima of the complex. The visible absorption spectra remained nearly constant throughout the irradiations with no λ_{max} changes and only slight intensity loss. At both wavelengths irradiated, the upper limit of the quantum yield, Φ , for the loss of reactant was $<5 \times 10^{-4}$ mol/einstein.

The low quantum yield fits with the previously observed pattern of Ru(II) ammine photosubstitution inertness when the MLCT state lies below the Ru(II) ligand field state. Furthermore, the low Φ indicates no loss in the integrity of the 2,2'-bipyrimidine bridge. These results satisfy the requirements for a highly absorbing nonreactive antenna metal fragment, which can be chelated to another metal complex through an effective energy-transfer bridge. In light of these results, research is currently in progress using the $(\text{NH}_3)_4\text{Ru}(\text{bpym})^{2+}$ antenna fragment coupled through the 2,2'-bipyrimidine to more reactive metal centers.

Acknowledgment. The authors thank the office of Basic Energy Science, Department of Energy, for support of this research (Contract No. DE-AS09-89ER10671). J.D.P. also acknowledges Johnson-Matthey, Inc., for loan of the ruthenium used in these studies and Professor Eric V. Dose, Department of Chemistry, University of Florida, for some helpful discussions.

Registry No. $(\text{NH}_3)_4\text{Ru}(\text{bpym})(\text{ClO}_4)_2$, 82583-14-0; $((\text{NH}_3)_4\text{Ru})_2(\text{bpym})(\text{ClO}_4)_4$, 82583-16-2; $[\text{Ru}(\text{NH}_3)_5\text{H}_2\text{O}](\text{TFMS})_3$, 53195-18-9.